Manuscript Category: Signaling & Cell biology (SCB)

$NRAS^{Q61K}$ melanoma tumor formation is reduced by p38-MAPK14 activation in zebrafish models and NRAS-mutated human melanoma cells

Ishani Banik[1], Phil F. Cheng[1], Christopher M. Dooley[2&3], Jana Travnickova[4], Munise Merteroglu[2&5], Reinhard Dummer[1], Elizabeth E. Patton[4], Elisabeth M. Busch-Nentwich[2&5*], Mitchell P. Levesque[1*]

1. University Hospital Zurich, University of Zurich, Zurich, Switzerland
2. Wellcome Sanger Institute, Hinxton, Cambridge, United Kingdom
3. Max Planck Institute for Developmental Biology, Tübingen, Germany
4. MRC Human Genetics Unit and Cancer Research UK Edinburgh Centre, MRC Institute of Genetics and Molecular Medicine, University of Edinburgh, Western General Hospital , Edinburgh, UK
5. Cambridge Institute of Therapeutic Immunology & Infectious Disease (CITIID), Department of Medicine, University of Cambridge, Cambridge, United Kingdom

*Corresponding authors: mitchell.levesque@usz.ch, emb81@medschl.cam.ac.uk

Corresponding author information: Mitch Levesque, Dept. of Dermatology, University of Zurich, Wagistrasse 14, 8952 Schlieren, Switzerland, phone: +41-(0) 43 253 3262, mitchell.levesque@usz.ch

Running title: p38α acts as tumor suppressor in NRAS mutant melanoma

Keywords: Zebrafish, melanoma, p38-MAPK14 pathway, NRAS mutation, ansiomycin

Conflict of interest: The authors declare no potential conflicts of interest.

Abstract

Oncogenic BRAF and NRAS mutations drive human melanoma initiation. We used transgenic zebrafish to model NRAS mutant melanoma and the rapid tumor onset allowed us to study candidate tumor suppressors. We identified P38α-MAPK14 as a potential tumor suppressor in The Cancer Genome Atlas melanoma cohort of NRAS mutant melanomas, and overexpression significantly increased the time to tumor onset in transgenic zebrafish with NRAS-driven melanoma. Pharmacological activation of P38α-MAPK14 using anisomycin reduced *in vitro* viability of melanoma cultures, which we confirmed by stable overexpression of p38α. We observed that the viability of MEK-inhibitor resistant melanoma cells could be

reduced by combined treatment of anisomycin and MEK-inhibition. Our study demonstrates that activating the p38α-MAPK14 pathway in the presence of oncogenic NRAS abrogates melanoma *in vitro* and *in vivo*.

Significance

The significance of our study is in the accountability of NRAS mutations in melanoma. We demonstrate here that activation of p38α-MAPK14 pathway can abrogate NRAS mutant melanoma which is contrary to the previously published role of p38α-MAPK14 pathway in BRAF mutant melanoma. These results implicate that BRAF and NRAS mutant melanoma may not be identical biologically. We also demonstrate the translational benefit of our study by using a small molecule compound-anisomycin (already in use for other diseases in clinical trials) to activate p38α-MAPK14 pathway.

Introduction

Melanoma arises from the acquisition of several sequential oncogenic events (Shain et al., 2016). The two most frequently mutated oncogenes in melanoma are BRAF and NRAS, in which activating mutations lead to constitutive signaling of the mitogen-activated protein kinase (MAPK) pathway and thereby enhance tumor growth and promote disease progression (Akbani et al., 2015; Davies et al., 2002; Platz, Egyhazi, Ringborg, & Hansson, 2008). Although several therapeutic options exist for melanoma, novel strategies targeting NRAS mutations are still at an exploratory stage. During development, highly conserved cues regulate pigment cell fate, mainly through the expression of the microphthalmia-associated transcription factor (MITF) (Widlund & Fisher, 2003). Melanoma models that express the activated human oncogenes $NRAS^{Q61K}$ or $BRAF^{V600E}$ under control of the *mitfa* promoter in zebrafish melanocytes have been powerful models to study the basic mechanisms of tumorigenesis. Previously, zebrafish have been used to generate *in vivo* models to simulate human naevi and melanoma (C. J. Ceol et al., 2011; Dovey, White, & Zon, 2009; Kaufman et al., 2016; Patton et al., 2005). Similar to (McConnell et al., 2019), we followed the approach of generating a rapid, transient *mitfa* promoter driven $NRAS^{Q61K}$ zebrafish melanoma model in *mitfa*^{w2};*tp53*^{zdf1} double mutants using the minicoopR vector and Tol2 transgenesis system.

To identify suppressors of NRAS-driven melanoma in humans, we analyzed The Cancer Genome Atlas, which revealed that P38α-MAPK14 is often gained in human melanomas with NRAS oncogenic mutations and loss-of-function p53. These patients survive longer than their peers do. P38α-MAPK14 overexpression *in vivo* significantly delayed the onset of $NRAS^{Q61K}$ driven melanoma, confirming its role as a tumor suppressor in this genetic background. We reproduced these results *in vitro* demonstrating that stable

overexpression of p38α-MAPK14, or pharmacological activation of p38α-MAPK14, was tumor suppressive in $NRAS^{Q61K}$ mutant patient-derived melanoma cultures.

Methods

In vivo experiments

Gateway entry clone pENTR5-mitf was created by PCR amplifying full length open reading frame using M24 Nac>Nac (Dorsky, Raible, & Moon, 2000) (gift from Randall Moon, Addgene plasmid # 17174) and ligated to pENTR5-TOPO activated vector (Invitrogen) according to manufacturer's instructions (Khosravi-Far et al., 1996). Gateway middle entry clones pmiddle-$NRAS^{Q61K}$ and pmiddle-MAPK14 was created by PCR amplifying full length open reading frame using pBabe N-Ras 61K (gift from Channing Der, Addgene plasmid # 12543) and pDONR223-MAPK14 (gift from William Hahn & David Root, Addgene plasmid # 23865) and ligated to pENTR/D-TOPO TA (Invitrogen) using manufacturer's instructions (Hao et al., 2007; Johannessen et al., 2010). The pENTR5-mCherry and the MiniCoopR destination vector were gifts from Dr. Alexa Burger and Dr. Craig Ceol respectively. Individual MiniCoopR clones were created by ligating the entry vector containing mitf promoter, either of the middle entry vectors and pENTR5-mCherry to the minicoopR destination vector using LR clonase under standard conditions (Invitrogen). Tol2mRNA transposase was created using the SP-6 primer and the PCS-TP vector (Kawakami et al., 2004) with the mMESSAGEmMachine kit (Ambion Inc) according to manufacturer's instructions. The pENTR5-mCherry was only used for its compatibility to fulfill the LR reaction. The middle entry clones containing the genes of interest were cloned with a stop codon at the end to prevent any m-Cherry expression. This had been done in order to avoid any abnormal expression of our genes of interest. Varying concentrations (60-100 ng/µl) of individual minicoopR vector along with 25 ng/µl of Tol2 mRNA transposase was microinjected into *mitfa*^{w2}*;tp53*^{zdf1} double mutant embryos at one cell stage. At larval stages post injection, embryos with rescued melanocytes were chosen for further assessment and scored weekly for presence of visible tumors. Zebrafish maintenance and genotyping protocols have been described in details in supplementary methods.

TCGA Methods

The results shown here are in whole or part based upon data generated by the TCGA Research Network: https://www.cancer.gov/tcga. No new genetic datasets were made. Publicly available SKCM TCGA data were downloaded with the TCGAbiolinks package (Cava et al., 2017). Patients with an oncogenic NRAS mutation, G12 or Q61, and with a p53 non-synonymous mutation and/or copy number loss were selected for further analysis. This cohort of patients was segregated into two groups: patients surviving less than 1

year, or patients surviving more than 1 year. The copy number GISTIC scores between these two groups were compared using a chi-squared test.

Immunohistochemistry

Zebrafish were euthanized and stored in 10 % formalin. Zebrafish were dissected and decalcified in 0.5 M EDTA, embedded in paraffin block and cut into 5 μm thick sections. The sections were then deparaffinized, rehydrated in decreasing concentrations of alcohol (99 %, 90 %, 70 %), bleached (3 %H_2O_2 and 1 %KOH) and antigen retrieved. 0.1 M citric acid (8.2 mM sodium citrate, pH 6) was used for mitf, Melan-A, pH3 and Sox10 while Tris-EDTA buffer (10 mM Tris, 1 mM EDTA, 0.05 % Tween 20, pH 9) was used for p38α and phospho-p38α. Serum free protein blocking (DAKO) was carried out for 30 minutes at room temperature and incubated with primary antibody overnight at 4 ^oC. After removal of primary antibody and washing with TBS buffer the slides were incubated with HRP rabbit/mouse secondary antibody and incubated for 30 minutes at room temperature followed by washing with TBS buffer. For visualization DAB chromogen:DAB substrate (DAKO 1:50) was used to reveal the HRP at room temperature followed by washing with water. The slides were then counter stained with haematoxylin for 4 minutes followed by washing and rinsing with water and acidic alcohol, blued up lithium chloride and finally dehydrating with increasing concentrations of alcohol (70 %, 90 %, 99 %) and washing in xylene. The slides were mounted using DPX mounting media and left to dry. Primary antibodies used were Mitf (Abcam 1:1500), Sox10 (Abcam 1:2500), Melan-A (DAKO 1:50), phospho-Histone 3 (Cell Signaling 1:200), p38α (Cell Signaling 1:800) and phospho-p38α (Cell Signaling 1:1000). Sections were imaged using Hamamatsu Nanozoomer XR slide scanner.

Cell lines and culture conditions

The patient-derived melanoma cell lines were provided by Melanoma Biobank, University Hospital Zurich, which were derived according to previously described methods (Raaijmakers et al. 2015) . All melanoma cell lines were cultured in RPMI1640 medium supplemented with 5 % fetal bovine serum and 2 mM L-glutamine and 50 mg/ml of Normocin (invivoGen). HEK293T cells were cultured in DMEM medium supplemented with 5 % fetal bovine serum and 2 mM L-glutamine. All cell lines were maintained at 37 ^oC in a humidified 5 % CO_2 atmosphere. Anisomycin and SP600125 was obtained from Cell Signaling. P38 inhibitor SB203580 was obtained from Selleckchem. MEK inhibitor trametinib was obtained from Novartis, Zurich.

Cell Viability assay

The growth inhibitory effect was tested under four different conditions- treatment with anisomycin, treatment with SB203580, treatment with MEK inhibitor-trametinib only, treatment with combination of anisomycin and trametinib. DMSO was used as the vehicle control for all the experiments. The cells were seeded at a density of 2 x 10^3 cells/well in a 96 well plate. 24 hours post seeding they were treated with either of the 4 conditions. After 72 hours of incubation the treated medium was aspirated and 100 µL of 1x Resazurin was added and incubated until color change was observed in the wells. Absorbance was measured at 490 nm using a microplate reader (Tecan, infinite M200Pro). Each experiment was performed with at least three biological replicates and repeated at least three times. IC50 calculations were made using GraphPad Prism and the synergy calculations were made using Synergyfinder.

DNA synthesis inhibition assay

The ability of anisomycin or SB203580 to inhibit cell proliferation was determined using BrdU colorimetric assay (Roche). The quantification of cell proliferation is based on the measurement of BrdU incorporation during DNA synthesis in proliferating cells. The cells were seeded at a density of 2 x 10^3 cells/well in a 96 well plate. 24 hours post seeding they were treated with anisomycin or SB203580. 72 hours post-treatment BrdU labelling solution, anti BrdU POD solution, washing solution and substrate solution was added according to manufacturer's instructions (Cell proliferation ELISA, BrdU colorimetric, Roche). Absorbance was measured at 370 nm using a plate reader (Tecan, infinite M200Pro). Each experiment was performed with three biological replicates and repeated at least three times.

P38α and phospho-p38α activation and inhibition

Cells were lysed with radioimmuno precipitation assay (RIPA) buffer (150 mM NaCl,15 mM $MgCl_2$,1 mM EDTA, 50 mM HEPES, 10 % glycerol, 1 % triton-X100, 1 tablet/mL each of phosphatase inhibitor and protease inhibitor) on ice for 30 minutes and 20 µg of protein were analyzed using standard western blotting. Protein quantification was done using standard Bradford assay. Cell lysates were collected 30 minutes post 0.1 µM/100 µM anisomycin treatment or 2 hours post 10 µM SB203580/SP600125 or 30 minutes pre-treatment with anisomycin followed by 2 hours treatment with SB203580/SP600125. P38α, phospho-p38α, total JNK, phospho-JNK, total ERK, phospho-ERK, total MEK and phospho-MEK (Cell Signaling) were used at 1:1000 dilution. Anti-hsp90 (Cell Signaling) was used as loading control at 1:1000 dilution. Following the probing of membrane for phospho-antibodies, they were stripped using stripping buffer (15 g glycine, 1 g SDS, 10 mL Tween20 in 1 L dd.H_20) followed by blocking and primary antibody incubation overnight. All membranes were probed for 60 minutes at room temperature with secondary anti-

rabbit antibody (Cell Signaling) at 1:2000 dilution. The visualization was performed using ECL chemifluorescent reagent (Invitrogen) or ECL-western bright Sirius/Quantum (Advantas).

Colony formation assay

Cells were seeded in 12 well plate at a density of 5 x 10^2, 1 x 10^3, 2 x 10^3 with 4 replicates and incubated at 37 ^{o}C. RPMI supplemented medium was re-freshed every 72 hours. The cell lines were incubated until colonies appeared within 10-15 days. For staining, 1 ml/well crystal violet (0.5 % w/v) dye was added and incubated for 20 minutes at room temperature on a shaker. Next, the plates were inverted and washed gently under running tap water. The plates were inverted and dried over night at room temperature. The plates were measured using EPSON scanner and analyzed using the Image J plugin-colony area (Guzman, Bagga, Kaur, Westermarck, & Abankwa, 2014).

Production of stably transduced cell lines overexpressing p38α-MAPK14

To create the vector containing p38α-MAPK14 driven by CMV promoter, the p38α-MAPK14 full length open reading frame was PCR amplified using primers F5'AGGGAGACCCAAGCTTGGTACCGGCACC3' and R5'TCAGGACTCCATCTCTTCTTGGTC3'. Addgene vector 62148 (Albers et al., 2015) with CMV promoter driving mCherry was used to restriction digest mCherry sequence with KpnI and SalI to create an open vector in order to replace the mCherry sequence with p38α sequence. Next, the PCR product with full length p38α sequence was ligated to open vector with CMV promoter using HiFi DNA Master Mix under standard conditions (NEB). This vector containing p38α-MAPK14 driven by CMV promoter was embedded in pMuLE Lenti Dest eGFP backbone co-expressing green fluorescent protein (GFP) (gift from Ian Frew, Addgene plasmid #62175) (Albers et al., 2015) using entry vector pMuLE ENTR MCS L5-L2 (gift from Ian Frew, Addgene plasmid #62085) in a site directed LR gateway reaction (Invitrogen). LR site directed gateway cloning was used in the same way to create mock vector expressing only GFP. Addgene vector 62084 (Albers et al., 2015) (gift from Ian Frew, Addgene plasmid #62084) was used instead of p38α entry vector as middle entry clone. Entry vectors 62084 and 62085 were re-combined with destination vector 62175 to create final expression vector as described above. The expression vector with p38α-MAPK14/mock-GFP, the packaging plasmid psPAX2 (Trono) and the envelope plasmid pMD2.G (Trono) were co-transfected with polyethylenimine (Polysciences) on HEK293T cells. 48 hours post transfection media containing lentiviral particles were added to melanoma cells in a 1:1 ratio with RPMI. The transduced cells were FACS-sorted for GFP before expanding.

Annexin-V/PI staining

Cell death to measure apoptosis was assayed using Annexin-V/PI kit (Invitrogen). Cells were seeded up to confluency in six well plates. On the day of treatment, the monolayer was collected, the cells were washed once with PBS and trypsinized. All supernatants including live and dead cells were collected before centrifuging for 5 minutes at 1500 rpm. Cells were re-suspended in 150 µL 1x binding buffer (10 mM HEPES, 140 mM NaCl, 2.5 mM $CaCl_2$, pH 7.4) in concentration of 1 x 10^6 cells/mL. 5 µL of PI/Annexin-V was added and incubated at room temperature in the dark for 20 minutes. Samples were transferred to ice and analyzed immediately on BD FACS AriaII. FloJo software was used for analysis.

Statistical Analysis and blinding approach

Results of *in vitro* experiments are presented as mean ± standard deviation or mean ± standard error representation of three independent experiments. Student t-test was used to compare continuous variables. Chi-squared test was used to measure categorical data, specifically to account for the different stages of apoptosis upon treatment with anisomycin in Figure 4. Median time to tumor formation was analyzed using Log rank test and Kaplan Meier method. P-value of less than 0.05 was considered statistically significant.
A partial blinding approach was followed for some of the experiments. The injection of plasmids, staining and analyzing of tissue section was performed by 2 people at 2 different time points. The tubes used to store the plasmids before injection and the slides for IHC were labelled with numbers only, eliminating gene names (such as NRAS or p38). One person in both the experiments was blinded.

Results

Tumor suppressive function of p38α in NRAS driven transgenic zebrafish melanoma

In order to study the oncogenic role of human $NRAS^{Q61K}$, we produced a transgenic model in zebrafish using the Tol-2 miniCoopR vector (Craig J. Ceol et al., 2011). We generated individual clones of human $NRAS^{Q61K}$ Tol-2 vectors and injected them into single cell *mitfa*^{w2};*tp53*^{zdf1} double loss-of-function mutants. In this system, candidate genes such as $NRAS^{Q61K}$ are physically coupled to the *mitfa* rescuing minigene. They are therefore expressed in rescued melanocytes, some of which will transform and develop into tumors (Iyengar, Houvras, & Ceol, 2012). We then monitored those fish with rescued melanocytes for one

year. We stained the tumor sections derived from euthanized, transgenic fish which were positive for the proliferation marker pH3 and classic melanoma markers such as Melan-A, MITF, and Sox10 (Figure 1A). Due to the very early onset of melanoma (i.e., 37 days) in the $NRAS^{Q61K}$ transgenic fish, they could not be mated. These data suggest that the $NRAS^{Q61K}$ oncogene generates aggressive melanoma tumors in zebrafish. Due to the histological similarity of zebrafish melanoma to human nodular/cutaneous melanoma and the rapid melanoma onset, we considered *mitfa* driven $NRAS^{Q61K}$ transgenic zebrafish to be an efficient tool for further mechanistic experiments (Patton et al., 2005) (Ceol, Houvras, White, & Zon, 2008).

Given the high medical need for therapies in NRAS-mutated melanomas, we analyzed the publicly available TCGA (https://www.cancer.gov/tcga) cohort of p53-mutated NRAS-mutant melanoma patients for potential tumor-suppressor genes. In order to identify copy number variants and differentially expressed genes, we classified the cohort based on survival time. We compared the genetic profiles of long survivors with (overall survival) O.S >1 year and short survivors with O.S <1 year (Figure 1B). There were several significant genes with copy number differences between these groups. To identify potential genes that could provide a protective role when overexpressed in NRAS-mutated melanomas, we considered only copy number gains that might suppress the rapid tumor onset observed in $NRAS^{Q61K}$ transgenic zebrafish. Furthermore, to ensure functional disease relevance, candidate gene selection was based on highly conserved genes, particulary those with ≥80 % sequence similarity to the *Danio rerio* genome (Supplementary Figure 2). P38α (i.e., MAPK14) was the most relevant cancer associated gene gained in long survivors and most importantly even lost in some short survivors (Figure 1C, p=0.037). P38 mitogen-activated protein kinases are a class of mitogen-activated protein kinases that are responsive to stress stimuli, such as heat and osmotic shock, cytokines, and UV irradiation and they are involved in cell differentiation, autophagy, and apoptosis. Four p38 MAP kinases, p38α (MAPK14), β (MAPK11), γ (MAPK12/ERK6), and δ (MAPK13/SAPK4), have been identified, and their functions in cancer remain elusive (Meng & Wu, 2013). The p38 pathway has been most frequently associated with a tumor suppressor function by negatively regulating cell survival and proliferation (Han & Sun, 2007). Although it has been suggested that modulating p38 or its downstream targets, PODXL and DEL-1 can serve as candidate therapeutics in melanoma (J. Wenzina et al., 2020), the role of p38α in melanoma is unclear and needs further investigation. We therefore hypothesized that p38α was a tumor suppressor in NRAS mutant melanoma. To test this, we engineered the miniCoopR vector to overexpress p38α and injected it into $mitfa^{w2};tp53^{zdf1}$ double mutant embryos along with the miniCoopR vector overexpressing $NRAS^{Q61K}$. We then screened the embryos for melanocytic rescue in larval stages and then monitored them for tumor development for one year. The onset of melanoma in $NRAS^{Q61K}$ transgenic zebrafish occurred very early, by 37 days, demonstrating the aggressiveness of NRAS mutant melanoma. Interestingly, 30.7 % of fish developed tumors in $Tg(mitfa{:}p38\alpha);Tg(mitfa{:}NRAS^{Q61K});mitfa^{w2};tp53^{zdf1}$ in comparison to 54.8 % in

Tg(mitfa:NRAS^{Q61K});mitfa^{w2};tp53^{zdf1} (Figure 1D). Of the 30.7 % fish that developed tumors in *Tg(mitfa:p38α);Tg(mitfa:NRAS^{Q61K});mitfa^{w2};tp53^{zdf1}*, the first tumor development was at 71 days (Figure 1D). We also confirmed the expression of p38α and phospho-p38α by immunohistochemistry on tumor/skin section excised from the euthanized, transgenic animals (Figure 1E-G). *Tg(mitfa:NRAS^{Q61K});mitfa^{w2};tp53^{zdf1}* had negligible amounts of p38α and phospho-p38α in the tumor sections (Figure 1E). *Tg(mitfa:p38α);mitfa^{w2};tp53^{zdf1}* did not develop any tumors nor did they show any abnormal disease related behavior (Figure 1F). Since these fish had melanocytic expression of p38α, immunohistochemistry revealed positive expression of p38α and phospho-p38α only in the epidermal sections of skin that consisted of melanocytes (Figure 1F).Tumor sections from *Tg(mitfa:p38α);Tg(mitfa:NRAS^{Q61K});mitfa^{w2};tp53^{zdf1}* had dramatically high levels of p38α and phospho-p38α (Figure 1G). Therefore, overexpression of p38α in zebrafish melanocytes bearing *mitfa*-restricted NRAS^{Q61K} had a survival benefit as measured by tumor free survival time by about 50 %. These combined data suggest that p38α is a tumor suppressor in the context of NRAS^{Q61K} zebrafish melanoma.

Overexpression of p38α induces tumor suppressive effects *in vitro*

In order to investigate if the observations made *in vivo* could be reproduced *in vitro,* we chose 6 patient-derived human melanoma cell cultures derived from tumors from different metastatic sites (i.e., 122102, 130107, 140805, 130227, 130429, and 160915 detailed in supplementary figure 1). To elucidate the role of p38α as a tumor suppressor, we stably transfected two patient-derived melanoma cell lines (130429 and 160915) to overexpress p38α. In addition, we also stably transfected the same cell lines to overexpress CMV-driven EGFP, which were labelled as EV (empty vector)_GFP_130429/160915. The cell lines that were transfected to overexpress p38α were labelled as p38α_GFP_130429/160915. The cell lines were probed for p38α and phospho-p38α with specific antibodies to confirm protein expression of p38α and phopsho-p38α with and without low doses of the p38 activator anisomycin (Figure 2A-B). To directly assess the role of p38α, on cell survival, we used resazurin assay to compare cell viability, which was significantly decreased in comparison to EV_GFP_130429/160915 (Figure 2C-D). Next, to monitor long-term effects of stable over-expression of p38α, we tested the ability of the transfected cells to form colonies using the colony formation assay. Consistent with the viability results, we observed reduced clonogenicity in the p38α transfected cell lines 130429 and 160915 compared to EV_GFP_130429/160915. The clonogenicity was measured by calculating the percentage of area covered by colonies formed (Figure 2E-F). The reduced cell viability and reduced clonogenicity could be attributed to either a reduction in cell proliferation or some form of cell death. We therefore performed an Annexin-V PI (Propidium iodide) death assay to check for apoptosis. Indeed, we found a significantly large proportion of early, late, and total apoptotic cells in the p38α overexpressing cell lines 130429 and 160915 (Figure 2G-H). In summary, tumor

suppressive functions, such as reduced clonogenicity and viability, appeared to be apoptosis-mediated in the stably transfected p38-α overexpressing cell lines 130429/160915. Overall, these data suggest an inhibitory effect of overexpression of p38α on NRAS mutant melanoma cells.

Pharmacological activation of p38α by anisomycin leads to tumor suppressive phenotypes *in vitro*

Our observations provided evidence that upregulation of the p38α-MAPK14 pathway could contribute to tumor suppressive functions. For this reason, we used anisomycin, which activates the p38α-MAPK14 pathway by phosphorylation of p38 (Hazzalin, Le Panse, Cano, & Mahadevan, 1998), while the pharmacological inhibitor SB203580 blocks the phosphorylation of p38 (Ana Cuenda et al., 1995). The levels of phospho-p38α were elevated when the six cell lines were treated with anisomycin, which could be reduced by treating the cells with the inhibitor SB203580 (Figure 3A, western blots). Therefore, the p38α-MAPK14 pathway could be modulated with the p38α activator anisomycin and the inhibitor SB203580 in all the patient-derived melanoma cell cultures used in this study. To examine the functional consequences on p38α-mediated cell survival, we determined cell viability using resazurin assays in the presence of anisomycin or SB203580. Treatment of melanoma cells with anisomycin resulted in reduced cell viability in a dose dependent manner as measured by the IC50 (half maximal inhibitory concentration) of all cell lines (Figure 3A). However, cell viability was not affected by SB203580 even up to a concentration of 1 µM. The IC50 of cells treated with anisomycin was at a low toxicity range between 0.2-0.3 µM while most cells had an IC50 ≥5 µM when treated with SB203580 (Figure 3A). Resazurin results were validated using BrdU colorimetric assays that measure the DNA synthesis of a cell. When the cells were stimulated with anisomycin, the incorporation of BrdU was dose dependently reduced in comparison to stimulation by SB203580, suggesting reduction of DNA synthesis under anisomycin treatment as measured by the IC50 values (Figure 3B). Overall, there was a significant change in cell viability and proliferation upon treatment with anisomycin as measured by both, resazurin and BrdU assays. These data show that cell viability and proliferation could be limited by activation of p38α suggesting a tumor suppressive role of p38α in NRAS mutant melanoma cells.

Activation of p38α by anisomycin mimics stable overexpression of p38α and re-sensitizes MEK inhibitor resistant cells to cell death

So far, our results clearly suggested that up-regulation of p38α in NRAS mutant cells had tumor suppressive effects. We next wanted to test whether the reduced melanoma cell viability upon anisomycin treatment was also due to an increase in apoptosis. For this reason, we performed Annexin-V PI assays after 72 hours of treatment with 0.1 µM anisomycin. Consistent with the results obtained earlier, treatment

with anisomycin induced a significantly higher rate of apoptosis in 122102, 130429 and 160915 compared to untreated cells (Figure 4A). Although not significant, 130227 cells had a 10 % increase in overall apoptosis when treated with anisomycin while 140805 did not have any significant change in apoptosis. Treated 130107 cells had a very high degree of apoptosis (>90 %) even without treatment, possibly due to their sensitivity to the staining dyes and incubation times for a FACS read-out. An account of early, late, and total apoptosis indicated that the late apoptosis population in anisomycin-treated cells is particularly high (Figure 4A). Taken, together these results show that tumor suppressive functions can be achieved by pharmacological activation of phospho-p38α with anisomycin and can be used as an alternative to stable transfection of p38α overexpression. More importantly, these results demonstrate that the consequence of high p38α in NRAS mutant melanoma cells either by genetically modifying cells to overexpress p38α or by using anisomycin is mostly apoptosis-mediated cell death.

In order to evaluate the use of anisomycin as a therapeutic agent to target melanoma cells, we compared its effectiveness to that of the commonly used MEK inhibitor trametinib. Cell viability was compared by using IC50 values attained after resazurin assays. All patient-derived melanoma cells collected at the University of Zurich Biobank are tested for drug sensitivity after expansion of cells *in vitro* in addition to comparing patient responses. Drug sensitive cell lines have IC50 of ≤0.1μM. All cell lines used in this study were considered to be drug resistant except for 130429. Indeed, from our experiments we observed that 130429 was MEKi sensitive and had the lowest IC50 value with trametinib treatment (Figure 4B, right). In contrast, all cell lines responded with reduced dose-response inhibition when treated with anisomycin as seen by a sigmoidal curve (Figure 4B, left). IC50 was in the range of 0.02-1μM in case of anisomycin treatment. Interestingly, the IC50 of the trametinib-sensitive cells 130429 was 0.04 μM compared to 0.02 μM with anisomycin. Therefore, as a single agent to reduce cell viability, anisomycin works more effectively than trametinib in all NRAS mutant melanoma cell lines used in this study. Lastly, to re-sensitize trametinib resistant melanoma cells, we co-treated the cells with anisomycin and trametinib with a concentration matrix ranging from 0.1-1000 nM. A synergy score was assigned to each value and is indicated by red color. A synergistic value was obtained for five cell lines when co-treated with anisomycin and trametinib in a low cytotoxicity range of 0.1-10 nM as indicated by red synergy zones (Figure 4C). Cell line 140805 did not show synergy. The dose-response matrix for each cell line can be found in Supplementary Figure 3. Therefore, anisomycin, when used either as a single agent or in combination with trametinib, resulted in a reduction of cell viability in most of the NRAS melanoma cell lines tested in this study. Thus, low dose anisomycin treatment in NRAS mutant melanoma cells sensitizes them to MEK-inhibition treatment.

Anisomycin induces p38 activation along with JNK activation

To understand the mechanism of action of the short-term effects of low and high dose anisomycin, we collected cell lysates 30 minutes post treatment with 0.1 µM and 100 µM anisomycin and probed for MAPK pathway proteins phospho-JNK, phospho-ERK, and phospho-MEK along with phospho-p38α. We found a positive correlation between phospho-p38α and phospho-JNK under both low and high dose anisomycin for five cell lines (Figure 5). (The NRAS mutation was lost in 140805 and this cell line was excluded from hereon). All cells had high phospho-p38α and high phospho-JNK with only a partial increase of phospho-ERK under low and high anisomycin treatment. The levels of phospho-MEK remained unchanged. The total protein levels of p38α, JNK, ERK and MEK remained unchanged (Figure 5). These results prompted us to inquire if phospho-p38α protein levels could be affected by JNK inhibition. Indeed, anisomycin induced phospho-p38α protein expression could be suppressed not only by the p38α inhibitor SB203580 but also by the JNK inhibitor SP600125 in 122102, 130227 and 130429 (Figure 6). However, in 130107 and 160915, the addition of SP600125 in combination with anisomycin increased the phospho-p38 protein levels. It should be kept in mind that 130107 and 160915 had elevated levels of phospho-JNK when treated with anisomycin indicating that activated states of p38α can bypass JNK inhibition and that JNK inhibition is not enough to restore the inactivated state of p38α. This also suggests that once activated, p38α follows different pathways and feedback loops. These results strongly suggest a partial co-activation of both phospho-JNK and phospho-p38α upon stimulation by anisomycin. Therefore, activation of the p38α pathway shows the involvement of the JNK pathway in some NRAS mutant melanoma cells.

Discussion

Our results demonstrate that NRAS mutations with p53 loss cause rapid onset of melanoma in zebrafish. The hyperpigmentation and accelerated tumor onset is comparable to observations made by (McConnell et al., 2019) in their mcr:NRAS^{Q61R} transgenic line. Similar results were previously reported in eGFP:NRAS transgenic zebrafish (Dovey et al., 2009). Fish with the NRAS^{Q61K} transgene *Tg(mitfa:NRAS^{Q61K});mitfa^{w2};tp53^{zdf1}* developed rapid melanoma, making it a suitable model to pursue the identification of tumor suppressors. The current standard of care for metastatic patients with NRAS driver mutations are immune-based therapies as first-line treatments, then cytotoxic chemotherapy such as carboplatin/paclitaxel (C/P), dacarbazine (DTIC) or temozolomide (TMZ) as a second-line treatment (Boespflug, Caramel, Dalle, & Thomas, 2017). Since there is no FDA approved targeted therapy for NRAS mutant melanoma patients, new studies are needed to investigate the role of tumor suppressors or oncogenes for the development of druggable targets in the MAPK pathway. This, combined with the establishment of a rapid melanoma model harboring NRAS mutations, paved the way for this study to be focused on finding candidate genes that might be tumor suppressors in NRAS melanoma. We used the TCGA cohort consisting of NRAS mutant melanoma patients with p53 null alleles to match the background

mutations in our zebrafish model. We stratified the cohort based on their survival and identified a candidate tumor suppressor gene, p38α-MAPK14. The role of p38α has been implicated in liver, prostate, breast, bladder, lung, thyroid, head and neck squamous cell carcinomas (Demuth et al., 2007; Elenitoba-Johnson et al., 2003; Esteva et al., 2004; Greenberg et al., 2002; Iyoda et al., 2003; Junttila et al., 2007; Khandrika et al., 2009; Koul, Pal, & Koul, 2013; Kumar et al., 2010; Park et al., 2003; Pomerance, Quillard, Chantoux, Young, & Blondeau, 2006; Tsai, Shiah, Lin, Wu, & Kuo, 2003). Mammalian p38 mitogen-activated protein kinases (MAPKs) are activated by a wide range of cellular stresses as well as in response to inflammatory cytokines (A. Cuenda & Rousseau, 2007). The p38α-MAPK14 pathway is involved in a number of physiological functions such as tissue invasion, protection against apoptotic cell death, unlimited replication potential, *de novo* angiogenesis and metastasis (Ambrosino & Nebreda, 2001). Depending on the cell type, p38α-MAPK14 can either induce progression or inhibition at G1/S transition by differential regulation of specific cyclin levels (cyclin A or D1) as well as by phosphorylation of the retinoblastoma protein (pRb), which is a hallmark of G1/S progression (Brancho et al., 2003) (Ambrosino & Nebreda, 2001). Overall, p38α plays various roles in normal conditions, but the role of p38α in solid tumors may be critical for tumor cell survival and metastasis and the mechanism of action of p38α needs to be further investigated.

Our data suggest that p38α acts as a tumor suppressor in our *in vivo* zebrafish melanoma model. In *mitfa*^{w2};*tp53*^{zdf1} double mutants that overexpress both NRAS^{Q61K} and p38α, the time to tumor onset was significantly increased. Furthermore, our results strongly suggest that p38α retains its tumor suppressive function *in vitro*. Stable transfection of human melanoma cells to overexpress p38α induced apoptosis-mediated cell death leading to reduced cell viability and clonogenicity. We confirmed the tumor suppressive and pro-apoptotic effects of p38α activation upon stable transfection of p38α that could be phenocopied by pharmacological activation using anisomycin.

High levels of p38α activity act through a negative feedback loop, where ERK signaling prevents tumorigenesis, which is in line with our findings (Estrada, Dong, & Ossowski, 2009). We also observed reduced phospho-ERK protein levels 24 hours post treatment with anisomycin in the cell lines 122102, 130107, 130227, 130429 and 160915 (Supplementary Figure 4) suggesting an abrogation of MAPK signaling. p38α plays a dual role as a mediator of cell survival or of cell death depending on the cell type and stimuli. While the tumor suppressive function of p38α has been described (Bradham & McClay, 2006; Hickson et al., 2006; Yao et al., 2008), its pro-oncogenic role has also been studied (Wagner & Nebreda, 2009). The dual role has been attributed to the initial, later, and metastatic stages of cancer (Huret, Dessen, & Bernheim, 2003). However, our investigation suggests a tumor suppressive role in NRAS driven melanoma.

In support of our model, we also found similar tumor suppressive effects upon the application of anisomycin to upregulate p38α. Here we showed that anisomycin induced activation of p38α leads to a reduction of cell viability (resazurin assay) and DNA synthesis in melanoma cells (BrdU assay) and most importantly, low dose anisomycin induces apoptosis-mediated cell death. Consistently, an earlier study showed that low doses of anisomycin could inhibit protein synthesis in melanoma cells by up to 30 %, which might result in a shift in the levels of the proteins involved in apoptosis (Slipicevic et al., 2013). The study also demonstrated that combined treatment of lexatumumab and anisomycin compared with lexatumumab alone significantly enhanced apoptosis in the melanoma cell lines-FEMX-1 and WM239.

P38α activation can be triggered by a variety of different stimuli and p38α activation is more likely to result in cell death. How it acts as a tumor suppressor in our model is yet to be determined in detail. Annexin V-PI assays in melanoma cell lines indicated that p38α overexpressing cells had a higher proportion of late apoptotic cells. P38α linked apoptosis has been reported to be mediated by caspase dependent and independent events particularly due to high ROS levels, high ATP, nutrient consumption and oxidative phosphorylation (Dolado et al., 2007; Trempolec et al., 2017). It has been demonstrated that p38 controls the regulation of checkpoint controls and cell cycle at G0, G1/S, and G2/M transition (Ambrosino & Nebreda, 2001).

The necessity of p38α for melanoma cell migration and proliferation was previously described by others (Estrada et al., 2009). Some studies revealed that inhibition of p38α activity and the subsequent phosphorylation of HSP27 by MAPKAP-K2 could prevent actin cytoskeleton reorganization necessary for cell migration (Hedges et al., 1999; Piotrowicz, Hickey, & Levin, 1998; Rousseau, Houle, Landry, & Huot, 1997). Our observations on the tumor sections obtained from *Tg(mitfa:p38α);Tg(mitfa:NRAS^{Q61K});mitfa^{w2};tp53^{zdf1}* revealed spindle shaped nuclei across the tumor suggesting a re-organized cytoskeleton in case of p38α expression (Supplementary Figure 5). Another study showed that changes in (extra-cellular matrix) ECM could lead to recruitment of T-cells (Kaur et al., 2019), a possible explanation for delay in tumor onset and a rearranged cytoskeleton in zebrafish over-expressing p38α. Matrix remodeling enzymes such as (matrix metalo-proteases) MMPs also regulate interaction between tumor cells and stroma. Inhibition of p38α-MAPK14 activity with SB203580 was shown to block MMP-9 expression in phorbol myristate acetate (PMA)-treated human squamous cell carcinoma (Simon, Goepfert, & Boyd, 1998).

Surprisingly, the positive correlation between high phospho-p38α and high phospho-JNK contrasts with a previously published study focused on BRAF mutant melanoma (Judith Wenzina et al., 2020). Although our findings suggest a tumor suppressive role of p38α in NRAS mutated melanoma, it might have a different role in a BRAF mutant background. The reduction in ERK levels and therefore MAPK signaling

(Supplementary Figure4) in high p38α cells led us to speculate that the normally uncontrolled conversion of GTP in melanoma cells can be limited. GTPase activating proteins (GAPS) such as neurofibromin, RASA1, RASA2, NF1 are crucial for hydrolysis of GTP to GDP and indeed we found that p38α and GTPase activating proteins SPRED1, RASA1,RASA2 and NF1 cluster together in NRAS mutant melanoma cohort (Supplementary Figure 6). Similar observations were made by (J. Tang et al., 2020) where loss of function mutations in NF1 and RASA2 were found in melanocytes along with gain/change of function mutation in NRAS.

Our attempt to find out if the patient-derived NRAS mutant melanoma cell lines could be sensitized to the MEK inhibitor-trametinib led to the identification of synergistic effects on melanoma cell lines when co-treated with anisomycin and trametinib. Low dose anisomycin as a single agent was more effective at reducing cell viability when compared to trametinib as indicated by the IC50 values at low cytotoxicity range. *In vivo* studies have (Z. Tang et al., 2012) shown that anisomycin has low toxicity and no significant side effects at physiological therapeutic doses. Although the cytotoxicity and long-term side effects of anisomycin need to be investigated, it could be a potential pharmacological candidate for melanoma patients harboring NRAS mutations. Single-agent MEK-inhibitor therapy has not been effective as a monotherapy in metastatic melanoma patients and thus, targeting P38α-MAPK14 could be an alternative.

Acknowledgements

We thank Nicola Goodwin (The Sanger Institute, Cambridge) for zebrafish husbandry. We thank Prof. Dr. Michael Krauthamer (University of Zürich), Dr. Remco van Doorn (University of Leiden) and Dr. Judith Wenzina (University of Vienna) for their useful insights on the project. We thank the biobank at the University Hospital Zurich for providing melanoma cell lines. We thank Andreas Dzung, Corrine Stoffel, Dr. Annalisa Saltari, Dr. Ossia Eichhof and Dr. Aizhan Tastanova for helping at various stages of the project (University of Zurich). This project has received funding from the European Union's Horizon 2020 research and innovation programme under the Marie Sklodowska-Curie grant agreement No 641458. The work carried out at the University of Edinburgh was partly funded by EEP, MRC HGU Programme (MC_UU_00007/9), European Research Council (ZF-MEL-CHEMBIO-648489), and L'Oreal-Melanoma Research Alliance (401181).

Figure Legends

Figure 1: Identification of candidate tumor suppressor gene and tumor suppressive functions of p38α in NRAS^{Q61K} transgenic zebrafish

A: Histological analysis of tumor sections derived from $NRAS^{Q61K}$ transgenic zebrafish stained for H&E, pH3, Melan-A, Mitf and Sox10. Scale bars, 50 µm B: Segregation of p53 null NRAS mutant TCGA cohort based on overall survival; short survivors O.S <1 year and long survivors O.S >1 year C: Bar plot showing different proportions of copy number variants between long and short survivors. Chi-squared test (p=0.037). D: Difference in median onset of tumor between *Tg(mitfa:p38);Tg(mitfa:NRAS^{Q61K});mitfa^{w2};tp53^{zdf1}* versus *Tg(mitfa:NRAS^{Q61K});mitfa^{w2};tp53^{zdf1}* versus *Tg(mitfa:p38);mitfa^{w2};tp53^{zdf1}*. Log rank test (P=0.0092) E: Histological analysis of tumor sections derived from *Tg(mitfa:NRAS^{Q61K});mitfa^{w2};tp53^{zdf1}* and stained for H&E, p38α and phospho-p38α F: Histological analysis of skin from *Tg(mitfa:p38);mitfa^{w2};tp53^{zdf1}* stained for H&E, p38α and phospho-p38α G: Histological analysis of tumor from *Tg(mitfa:p38);Tg(mitfa:NRAS^{Q61K});mitfa^{w2};tp53^{zdf1}* stained for H&E, p38α and phospho-p38α. Stainings are representative sections from three animals except *Tg(mitfa:p38);mitfa^{w2};tp53^{zdf1}*. Scale bars, 80 µm.

Figure 2: Up-regulation of p38α by stable transfection induces apoptosis-mediated cell death resulting in reduced cell viability and clonogenicity in cell line 130429 and 160915

A-B: Relative protein expression of p38α and phospho-p38α in wt, EV_GFP and p38_GFP in 130429 and 160915 respectively. n≥3 independent experiments C-D: Cell lines 130429 and 160915 stably transfected to express p38α have significantly reduced cell viability compared to cells stably transfected to express GFP respectively as measured using Resazurin assay on day 3 . Each data point in C&D represents an average of 30 values per condition per independent experiment. Error bars represent standard error of the mean. Statistical tests done using two tailed unpaired student's t test and significance values indicated are: p ≤0.05 *, p ≤0.01 **, p ≤0.001 * * * E-F: Significant difference (p <0.001) in the area covered by colonies in cell line 130429 and 160915 stably expressing p38α compared to cells stably expressing GFP respectively. Beside are representative pictures of the colonies formed. n ≥3 independent experiments. Error bars represent standard error of the mean. Statistical tests done using two tailed paired student's t test and significance values indicated are: p ≤0.05 *, p ≤0.01 **, p ≤0.001 * * *. G-H: Significantly higher population of cells undergoing early, late and total apoptosis in cell line 130429 and 160915 stably transfected to express p38α compared to its mock GFP counterpart respectively. Total apoptosis was calculated as the sum of early, late apoptosis and necrosis. n ≥3 independent experiments. Error bars represent standard error of the mean. Statistical tests done using two tailed paired student's t test and significance values indicated are: p ≤0.05 *, p ≤0.01 **, p ≤0.001 * * *

Figure 3: Activation and inhibition of phospho-p38α by anisomycin and SB203580 respectively and reduction in cell viability and proliferation upon anisomycin treatment in all cell lines

A: Resazurin assay showing dose-dependent reduction in cell viability with increasing concentrations of anisomycin but not SB203580 as indicated by the IC50 values (in µM). Each data point represents an average of 3 values per condition per independent experiment. n ≥3 independent experiments. Error bars represent standard error of the mean. Below: Western blots showing activation and inhibition of phospho-p38α when stimulated by anisomycin and SB203580 in respective cell lines. B: BrdU colorimetric assay showing dose dependent reduction in incorporation of BrdU with increasing concentrations of anisomycin but not SB203580 as indicated by the IC50 values (in µM). Each data point represents an average of 3 values per condition per independent experiment. n ≥3 independent experiments. Error bars represent standard error of the mean.

Figure 4: Low dose anisomycin induces apoptosis-mediated cell death in NRAS mutant melanoma cell lines and shows synergistic effects with MEK inhibitor-trametinib

A: Annexin V-PI assay demonstrating significantly higher apoptosis rate in anisomycin (0.1 µM) treated 122102, 130429, 160915 compared to untreated cells. Anisomycin (0.1 µM) treated 130227 had 10 % higher apoptosis compared to untreated cells. Below: Separation of untreated and anisomycin treated cells into early apoptosis Q1, late apoptosis Q2, necrosis Q3 and live cells Q4. Error bars represent standard error of the mean. n ≥3 independent experiments. Statistical tests done using Chi-squared test and significance values indicated are: p ≤0.05 *, p ≤0.01 **, p ≤0.001 * * * B: Resazurin assay upon dose dependent treatment with anisomycin/trametinib. Sensitivity to the drug is measured by IC50 value in the table below. Each data point represents an average of 3 values per condition per independent experiment. n ≥3 independent experiments. Error bars represent standard error of the mean. Undetermined IC50 is indicated by 0.000 C: Synergy plots of 122102, 130107, 130227, 130429 , 140805 and 160915 treated with trametinib (concentrations on x-axis) and anisomycin (concentrations on y-axis). Red, white and green indicate synergistic, non- synergistic and antagonistic effects respectively. Each data point represents an average of 3 values per condition per independent experiment. n ≥3 independent experiments.

Figure 5: Anisomycin upregulates phospho-JNK along with phospho-p38α and JNK inhibitor SP600125 can suppress anisomycin induced p38α activation

Relative protein level expression of 122102, 130107, 130227, 130429 and 160915 under high (100 µM) and low (0.1 µM) dose anisomycin probed for phospho-p38α/p38α, phospho-JNK/JNK, phospho-ERK/ ERK and phospho-MEK/ with hsp90 as loading control.

Figure 6: p38 inhibitor-SB203580 and JNK inhibitor-SP600125 can suppress anisomycin induced p38α activation

Relative protein level expression of 122102, 130107, 130227, 130429 and 160915 under low (0.1 uM) dose anisomycin probed for phospho-p38α/p38α with hsp90 as loading control. Phospho-p38α levels were reduced when co-treated with anisomycin and SP600125 in 122102, 130227 and 130429 while phospho-p38α levels were reduced when co-treated with anisomycin and SB203580 in 122102,130107, 130227, 130429 and 160915. 130107 and 160915 had higher expression of phospho-p38α when co-treated with anisomycin and SP600125. On the right: Fold expression of p38α and phospho-p38α normalized to hsp90.

Supplementary Figure 1: Information on patient derived melanoma cell lines

Supplementary Figure 2: Genes with CNV gains and losses of short and long survivors with more than 80 % homology to *Danio rerio* genome.

Supplementary Figure 3: Dose-response matrix of synergistic effects of anisomycin and trametinib.

Supplementary Figure 4: Relative protein level expression of 122102, 130107, 130227, 130429 and 160915 under low (0.1 uM) dose anisomycin at 30 minutes and 24 hours probed for phospho-ERK/ERK, phospho-p38α/p38α, phospho-MEK/MEK and phospho-JNK/JNK with hsp90 as loading control. Phospho-ERK, phospho-p38 and phospho-JNK expression is reduced within 24 hours of anisomycin treatment in comparison to 30 minutes post treatment. Phospho-MEK and total p38, ERK, JNK, MEK levels remain unchanged.

Supplementary Figure 5: Tumor sections of *Tg(mitfa:NRAS^{Q61K});mitfa^{w2};tp53^{zdf1}* and *Tg(mitfa:p38);Tg(mitfa:NRAS^{Q61K});mitfa^{w2};tp53^{zdf1}* showing spindle shaped nuclei in the latter.

Supplementary Figure 6: Heatmap of RNA expression of MAPK14 with RASA1, RASA2, NF1 and SPRED1 in NRAS mutant melanoma patient cohort. On the right: Z score of normalized counts per million.

References

Akbani, R., Akdemir, Kadir C., Aksoy, B. A., Albert, M., Ally, A., Amin, Samirkumar B., & *al., e.* (2015). Genomic Classification of Cutaneous Melanoma. *Cell, 161*(7), 1681-1696. doi:https://doi.org/10.1016/j.cell.2015.05.044

Albers, J., Danzer, C., Rechsteiner, M., Lehmann, H., Brandt, L. P., Hejhal, T., . . . Frew, I. J. (2015). A versatile modular vector system for rapid combinatorial mammalian genetics. *J Clin Invest, 125*(4), 1603-1619. doi:10.1172/jci79743

Ambrosino, C., & Nebreda, A. R. (2001). Cell cycle regulation by p38 MAP kinases. *Biol Cell, 93*(1-2), 47-51.

Boespflug, A., Caramel, J., Dalle, S., & Thomas, L. (2017). Treatment of NRAS-mutated advanced or metastatic melanoma: rationale, current trials and evidence to date. *Ther Adv Med Oncol, 9*(7), 481-492. doi:10.1177/1758834017708160

Bradham, C., & McClay, D. R. (2006). p38 MAPK in development and cancer. *Cell Cycle, 5*(8), 824-828. doi:10.4161/cc.5.8.2685

Brancho, D., Tanaka, N., Jaeschke, A., Ventura, J. J., Kelkar, N., Tanaka, Y., . . . Davis, R. J. (2003). Mechanism of p38 MAP kinase activation in vivo. *Genes Dev, 17*(16), 1969-1978. doi:10.1101/gad.1107303

Cava, C., Colaprico, A., Bertoli, G., Graudenzi, A., Silva, T. C., Olsen, C., . . . Castiglioni, I. (2017). SpidermiR: An R/Bioconductor Package for Integrative Analysis with miRNA Data. *Int J Mol Sci, 18*(2). doi:10.3390/ijms18020274

Ceol, C. J., Houvras, Y., Jane-Valbuena, J., Bilodeau, S., Orlando, D. A., Battisti, V., . . . Zon, L. I. (2011). The histone methyltransferase SETDB1 is recurrently amplified in melanoma and accelerates its onset. *Nature, 471*(7339), 513-517. doi:10.1038/nature09806

Ceol, C. J., Houvras, Y., Jane-Valbuena, J., Bilodeau, S., Orlando, D. A., Battisti, V., . . . Zon, L. I. (2011). The histone methyltransferase SETDB1 is recurrently amplified in melanoma and accelerates its onset. *Nature, 471*(7339), 513-517. doi:10.1038/nature09806

Ceol, C. J., Houvras, Y., White, R. M., & Zon, L. I. (2008). Melanoma biology and the promise of zebrafish. *Zebrafish, 5*(4), 247-255. doi:10.1089/zeb.2008.0544

Cuenda, A., Rouse, J., Doza, Y. N., Meier, R., Cohen, P., Gallagher, T. F., . . . Lee, J. C. (1995). SB 203580 is a specific inhibitor of a MAP kinase homologue which is stimulated by cellular stresses and interleukin-1. *FEBS Letters, 364*(2), 229-233. doi:https://doi.org/10.1016/0014-5793(95)00357-F

Cuenda, A., & Rousseau, S. (2007). p38 MAP-kinases pathway regulation, function and role in human diseases. *Biochim Biophys Acta, 1773*(8), 1358-1375. doi:10.1016/j.bbamcr.2007.03.010

Davies, H., Bignell, G. R., Cox, C., Stephens, P., Edkins, S., Clegg, S., . . . Futreal, P. A. (2002). Mutations of the BRAF gene in human cancer. *Nature, 417*(6892), 949-954. doi:10.1038/nature00766

Demuth, T., Reavie, L. B., Rennert, J. L., Nakada, M., Nakada, S., Hoelzinger, D. B., . . . Berens, M. E. (2007). MAP-ing glioma invasion: mitogen-activated protein kinase kinase 3 and p38 drive glioma invasion and progression and predict patient survival. *Mol Cancer Ther, 6*(4), 1212-1222. doi:10.1158/1535-7163.Mct-06-0711

Dolado, I., Swat, A., Ajenjo, N., De Vita, G., Cuadrado, A., & Nebreda, A. R. (2007). p38α MAP Kinase as a Sensor of Reactive Oxygen Species in Tumorigenesis. *Cancer Cell, 11*(2), 191-205. doi:https://doi.org/10.1016/j.ccr.2006.12.013

Dorsky, R. I., Raible, D. W., & Moon, R. T. (2000). Direct regulation of nacre, a zebrafish MITF homolog required for pigment cell formation, by the Wnt pathway. *Genes Dev, 14*(2), 158-162.

Dovey, M., White, R. M., & Zon, L. I. (2009). Oncogenic NRAS cooperates with p53 loss to generate melanoma in zebrafish. *Zebrafish, 6*(4), 397-404. doi:10.1089/zeb.2009.0606

Elenitoba-Johnson, K. S., Jenson, S. D., Abbott, R. T., Palais, R. A., Bohling, S. D., Lin, Z., . . . Lim, M. S. (2003). Involvement of multiple signaling pathways in follicular lymphoma transformation: p38-mitogen-activated protein kinase as a target for therapy. *Proc Natl Acad Sci U S A, 100*(12), 7259-7264. doi:10.1073/pnas.1137463100

Esteva, F. J., Sahin, A. A., Smith, T. L., Yang, Y., Pusztai, L., Nahta, R., . . . Bacus, S. S. (2004). Prognostic significance of phosphorylated P38 mitogen-activated protein kinase and HER-2 expression in lymph node-positive breast carcinoma. *Cancer, 100*(3), 499-506. doi:10.1002/cncr.11940

Estrada, Y., Dong, J., & Ossowski, L. (2009). Positive crosstalk between ERK and p38 in melanoma stimulates migration and in vivo proliferation. *22*(1), 66-76. doi:10.1111/j.1755-148X.2008.00520.x

Greenberg, A. K., Basu, S., Hu, J., Yie, T. A., Tchou-Wong, K. M., Rom, W. N., & Lee, T. C. (2002). Selective p38 activation in human non-small cell lung cancer. *Am J Respir Cell Mol Biol, 26*(5), 558-564. doi:10.1165/ajrcmb.26.5.4689

Guzman, C., Bagga, M., Kaur, A., Westermarck, J., & Abankwa, D. (2014). ColonyArea: an ImageJ plugin to automatically quantify colony formation in clonogenic assays. *PLoS One, 9*(3), e92444. doi:10.1371/journal.pone.0092444

Han, J., & Sun, P. (2007). The pathways to tumor suppression via route p38. *Trends in biochemical sciences, 32*(8), 364-371. doi:10.1016/j.tibs.2007.06.007

Hao, H., Muniz-Medina, V. M., Mehta, H., Thomas, N. E., Khazak, V., Der, C. J., & Shields, J. M. (2007). Context-dependent roles of mutant B-Raf signaling in melanoma and colorectal carcinoma cell growth. *Mol Cancer Ther, 6*(8), 2220-2229. doi:10.1158/1535-7163.MCT-06-0728

Hazzalin, C. A., Le Panse, R., Cano, E., & Mahadevan, L. C. (1998). Anisomycin selectively desensitizes signalling components involved in stress kinase activation and fos and jun induction. *Molecular and cellular biology, 18*(4), 1844-1854. doi:10.1128/mcb.18.4.1844

Hedges, J. C., Dechert, M. A., Yamboliev, I. A., Martin, J. L., Hickey, E., Weber, L. A., & Gerthoffer, W. T. (1999). A role for p38(MAPK)/HSP27 pathway in smooth muscle cell migration. *J Biol Chem, 274*(34), 24211-24219. doi:10.1074/jbc.274.34.24211

Hickson, J. A., Huo, D., Vander Griend, D. J., Lin, A., Rinker-Schaeffer, C. W., & Yamada, S. D. (2006). The p38 kinases MKK4 and MKK6 suppress metastatic colonization in human ovarian carcinoma. *Cancer Res, 66*(4), 2264-2270. doi:10.1158/0008-5472.CAN-05-3676

Huret, J. L., Dessen, P., & Bernheim, A. (2003). Atlas of Genetics and Cytogenetics in Oncology and Haematology, year 2003. *Nucleic Acids Res, 31*(1), 272-274. doi:10.1093/nar/gkg126

Iyengar, S., Houvras, Y., & Ceol, C. J. (2012). Screening for melanoma modifiers using a zebrafish autochthonous tumor model. *Journal of visualized experiments : JoVE*(69), e50086-e50086. doi:10.3791/50086

Iyoda, K., Sasaki, Y., Horimoto, M., Toyama, T., Yakushijin, T., Sakakibara, M., . . . Hayashi, N. (2003). Involvement of the p38 mitogen-activated protein kinase cascade in hepatocellular carcinoma. *Cancer, 97*(12), 3017-3026. doi:10.1002/cncr.11425

Johannessen, C. M., Boehm, J. S., Kim, S. Y., Thomas, S. R., Wardwell, L., Johnson, L. A., . . . Garraway, L. A. (2010). COT drives resistance to RAF inhibition through MAP kinase pathway reactivation. *Nature, 468*(7326), 968-972. doi:10.1038/nature09627

Junttila, M. R., Ala-Aho, R., Jokilehto, T., Peltonen, J., Kallajoki, M., Grenman, R., . . . Kahari, V. M. (2007). p38alpha and p38delta mitogen-activated protein kinase isoforms regulate invasion and growth of head and neck squamous carcinoma cells. *Oncogene, 26*(36), 5267-5279. doi:10.1038/sj.onc.1210332

Kaufman, C. K., Mosimann, C., Fan, Z. P., Yang, S., Thomas, A. J., Ablain, J., . . . Zon, L. I. (2016). A zebrafish melanoma model reveals emergence of neural crest identity during melanoma initiation. *Science, 351*(6272), aad2197. doi:10.1126/science.aad2197

Kaur, A., Ecker, B. L., Douglass, S. M., Kugel, C. H., 3rd, Webster, M. R., Almeida, F. V., . . . Weeraratna, A. T. (2019). Remodeling of the Collagen Matrix in Aging Skin Promotes Melanoma Metastasis and Affects Immune Cell Motility. *Cancer Discov, 9*(1), 64-81. doi:10.1158/2159-8290.CD-18-0193

Kawakami, K., Takeda, H., Kawakami, N., Kobayashi, M., Matsuda, N., & Mishina, M. (2004). A Transposon-Mediated Gene Trap Approach Identifies Developmentally Regulated Genes in Zebrafish. *Developmental Cell, 7*(1), 133-144. doi:https://doi.org/10.1016/j.devcel.2004.06.005

Khandrika, L., Lieberman, R., Koul, S., Kumar, B., Maroni, P., Chandhoke, R., . . . Koul, H. K. (2009). Hypoxia-associated p38 mitogen-activated protein kinase-mediated androgen receptor activation and increased HIF-1alpha levels contribute to emergence of an aggressive phenotype in prostate cancer. *Oncogene, 28*(9), 1248-1260. doi:10.1038/onc.2008.476

Khosravi-Far, R., White, M. A., Westwick, J. K., Solski, P. A., Chrzanowska-Wodnicka, M., Van Aelst, L., . . . Der, C. J. (1996). Oncogenic Ras activation of Raf/mitogen-activated protein kinase-independent pathways is sufficient to cause tumorigenic transformation. *Molecular and cellular biology, 16*(7), 3923-3933. doi:10.1128/mcb.16.7.3923

Koul, H. K., Pal, M., & Koul, S. (2013). Role of p38 MAP Kinase Signal Transduction in Solid Tumors. *Genes & cancer, 4*(9-10), 342-359. doi:10.1177/1947601913507951

Kumar, B., Koul, S., Petersen, J., Khandrika, L., Hwa, J. S., Meacham, R. B., . . . Koul, H. K. (2010). p38 mitogen-activated protein kinase-driven MAPKAPK2 regulates invasion of bladder cancer by modulation of MMP-2 and MMP-9 activity. *Cancer Res, 70*(2), 832-841. doi:10.1158/0008-5472.Can-09-2918

McConnell, A. M., Mito, J. K., Ablain, J., Dang, M., Formichella, L., Fisher, D. E., & Zon, L. I. (2019). Neural crest state activation in NRAS driven melanoma, but not in NRAS-driven melanocyte expansion. *Dev Biol, 449*(2), 107-114. doi:10.1016/j.ydbio.2018.05.026

Meng, F., & Wu, G. (2013). Is p38γ MAPK a metastasis-promoting gene or an oncogenic property-maintaining gene? *Cell cycle (Georgetown, Tex.), 12*(14), 2329-2330. doi:10.4161/cc.25333

Park, J. I., Lee, M. G., Cho, K., Park, B. J., Chae, K. S., Byun, D. S., . . . Chi, S. G. (2003). Transforming growth factor-beta1 activates interleukin-6 expression in prostate cancer cells through the synergistic collaboration of the Smad2, p38-NF-kappaB, JNK, and Ras signaling pathways. *Oncogene, 22*(28), 4314-4332. doi:10.1038/sj.onc.1206478

Patton, E. E., Widlund, H. R., Kutok, J. L., Kopani, K. R., Amatruda, J. F., Murphey, R. D., . . . Zon, L. I. (2005). BRAF mutations are sufficient to promote nevi formation and cooperate with p53 in the genesis of melanoma. *Curr Biol, 15*(3), 249-254. doi:10.1016/j.cub.2005.01.031

Piotrowicz, R. S., Hickey, E., & Levin, E. G. (1998). Heat shock protein 27 kDa expression and phosphorylation regulates endothelial cell migration. *FASEB J, 12*(14), 1481-1490. doi:10.1096/fasebj.12.14.1481

Platz, A., Egyhazi, S., Ringborg, W., & Hansson, J. (2008). Human cutaneous melanoma; a review of NRAS and BRAF mutation frequencies in relation to histogenetic subclass and body site. *Molecular Oncology, 1*(4), 395-405. doi:10.1016/j.molonc.2007.12.003

Pomerance, M., Quillard, J., Chantoux, F., Young, J., & Blondeau, J. P. (2006). High-level expression, activation, and subcellular localization of p38-MAP kinase in thyroid neoplasms. *J Pathol, 209*(3), 298-306. doi:10.1002/path.1975

Raaijmakers, M.I.G., Widmer, D.S., Maudrich, M., Koch, T., Langer, A., Flace, A., Schnyder, C., Dummer, R., & Levesque, M.P. (2015). A new live-cell biobank workflow efficiently recovers heterogeneous melanoma cells from native biopsies. *Exp Derm, 24(5):377-80. doi:10.1111/exd.12683*

Rousseau, S., Houle, F., Landry, J., & Huot, J. (1997). p38 MAP kinase activation by vascular endothelial growth factor mediates actin reorganization and cell migration in human endothelial cells. *Oncogene, 15*(18), 2169-2177. doi:10.1038/sj.onc.1201380

Shain, A. H., Yu, R., Yeh, I., Benhamida, J., Kovalyshyn, I., Sriharan, A., . . . Bastian, B. (2016). Abstract 2372: The genetic evolution of melanoma. *76*(14 Supplement), 2372-2372. doi:10.1158/1538-7445.AM2016-2372 %J Cancer Research

Simon, C., Goepfert, H., & Boyd, D. (1998). Inhibition of the p38 mitogen-activated protein kinase by SB 203580 blocks PMA-induced Mr 92,000 type IV collagenase secretion and in vitro invasion. *Cancer Res, 58*(6), 1135-1139.

Slipicevic, A., Oy, G. F., Rosnes, A. K., Stakkestad, O., Emilsen, E., Engesaeter, B., . . . Florenes, V. A. (2013). Low-dose anisomycin sensitizes melanoma cells to TRAIL induced apoptosis. *Cancer Biol Ther, 14*(2), 146-154. doi:10.4161/cbt.22953

Tang, J., Fewings, E., Chang, D., Zeng, H., Liu, S., Jorapur, A., . . . Shain, A. H. (2020). The genomic landscapes of individual melanocytes from human skin. 2020.2003.2001.971820. doi:10.1101/2020.03.01.971820 %J bioRxiv

Tang, Z., Xing, F., Chen, D., Yu, Y., Yu, C., Di, J., & Liu, J. (2012). In vivo toxicological evaluation of Anisomycin. *Toxicol Lett, 208*(1), 1-11. doi:10.1016/j.toxlet.2011.10.001

Trempolec, N., Munoz, J. P., Slobodnyuk, K., Marin, S., Cascante, M., Zorzano, A., & Nebreda, A. R. (2017). Induction of oxidative metabolism by the p38alpha/MK2 pathway. *Sci Rep, 7*(1), 11367. doi:10.1038/s41598-017-11309-7

Trono, D. Addgene plasmid # 12259 ; http://n2t.net/addgene:12259 ; RRID:Addgene_12259.

Trono, D. Addgene plasmid # 12260 ; http://n2t.net/addgene:12260 ; RRID:Addgene_12260.

Tsai, P. W., Shiah, S. G., Lin, M. T., Wu, C. W., & Kuo, M. L. (2003). Up-regulation of vascular endothelial growth factor C in breast cancer cells by heregulin-beta 1. A critical role of p38/nuclear factor-kappa B signaling pathway. *J Biol Chem, 278*(8), 5750-5759. doi:10.1074/jbc.M204863200

Wagner, E. F., & Nebreda, A. R. (2009). Signal integration by JNK and p38 MAPK pathways in cancer development. *Nat Rev Cancer, 9*(8), 537-549. doi:10.1038/nrc2694

Wenzina, J., Holzner, S., Puujalka, E., Cheng, P. F., Forsthuber, A., Neumüller, K., . . . Petzelbauer, P. (2020). Inhibition of p38/MK2 Signaling Prevents Vascular Invasion of Melanoma. *J Invest Dermatol, 140*(4), 878-890.e875. doi:10.1016/j.jid.2019.08.451

Wenzina, J., Holzner, S., Puujalka, E., Cheng, P. F., Forsthuber, A., Neumüller, K., . . . Petzelbauer, P. (2020). Inhibition of p38/MK2 Signaling Prevents Vascular Invasion of Melanoma. *Journal of Investigative Dermatology, 140*(4), 878-890.e875. doi:https://doi.org/10.1016/j.jid.2019.08.451

Widlund, H. R., & Fisher, D. E. (2003). Microphthalamia-associated transcription factor: a critical regulator of pigment cell development and survival. *Oncogene, 22*(20), 3035-3041. doi:10.1038/sj.onc.1206443

Yao, Y. Q., Ding, X., Jia, Y. C., Huang, C. X., Wang, Y. Z., & Xu, Y. H. (2008). Anti-tumor effect of beta-elemene in glioblastoma cells depends on p38 MAPK activation. *Cancer Lett, 264*(1), 127-134. doi:10.1016/j.canlet.2008.01.049

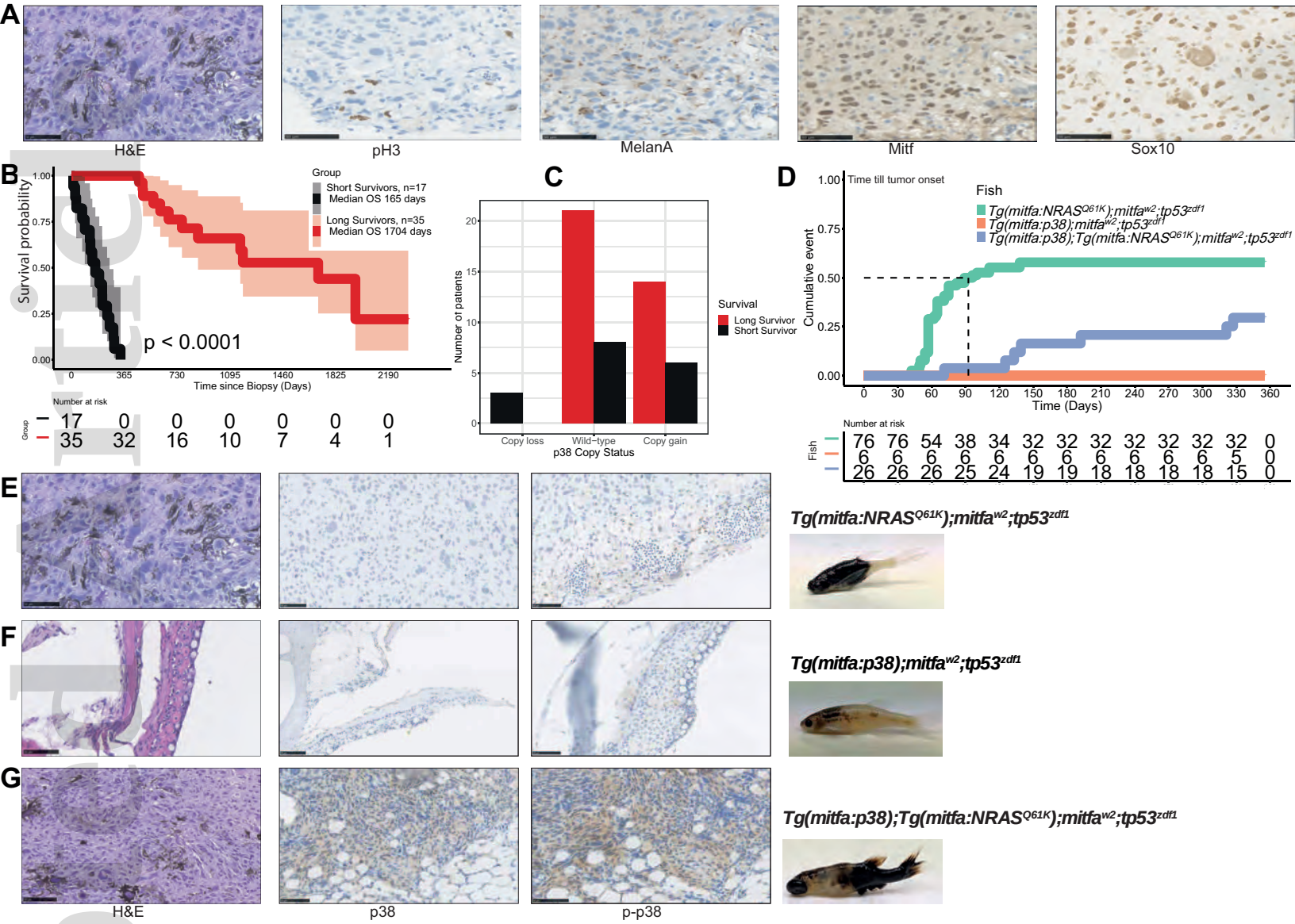

Figure 1: Identification of candidate tumor suppressor gene and tumor suppressive functions of p38α in NRAS^{Q61K} transgenic zebrafish

A: Histological analysis of tumor sections derived from NRAS^{Q61K} transgenic zebrafish stained for H&E, pH3, Melan-A, Mitf and Sox10. Scale bars, 50μm B: Segregation of p53 null NRAS mutant TCGA cohort based on overall survival; short survivors O.S<1 year and long survivors O.S>1 year C: Bar plot showing different proportions of copy number variants between long and short survivors. Chi-squared test (p=0.037). D: Difference in median onset of tumor between ***Tg(mitfa:p38);Tg(mitfa:NRAS^{Q61K});mitfa^{w2};tp53^{zdf1}*** versus ***Tg(mitfa:NRAS^{Q61K});mitfa^{w2};tp53^{zdf1}*** versus ***Tg(mitfa:p38);mitfa^{w2};tp53^{zdf1}***. Log rank test (P=0.0092) E: Histological analysis of tumor sections derived from ***Tg(mitfa:NRAS^{Q61K});mitfa^{w2};tp53^{zdf1}*** and stained for H&E, p38α and phospho-p38α F: Histological analysis of skin from ***Tg(mitfa:p38);mitfa^{w2};tp53^{zdf1}*** stained for H&E, p38α and phospho-p38α G: Histological analysis of tumor from ***Tg(mitfa:p38);Tg(mitfa:NRAS^{Q61K});mitfa^{w2};tp53^{zdf1}*** stained for H&E, p38α and phospho-p38α. Stainings are representative sections from three animals except ***Tg(mitfa:p38);mitfa^{w2};tp53^{zdf1}***. Scale bars, 80 μm.

pcmr_12925_f1.eps

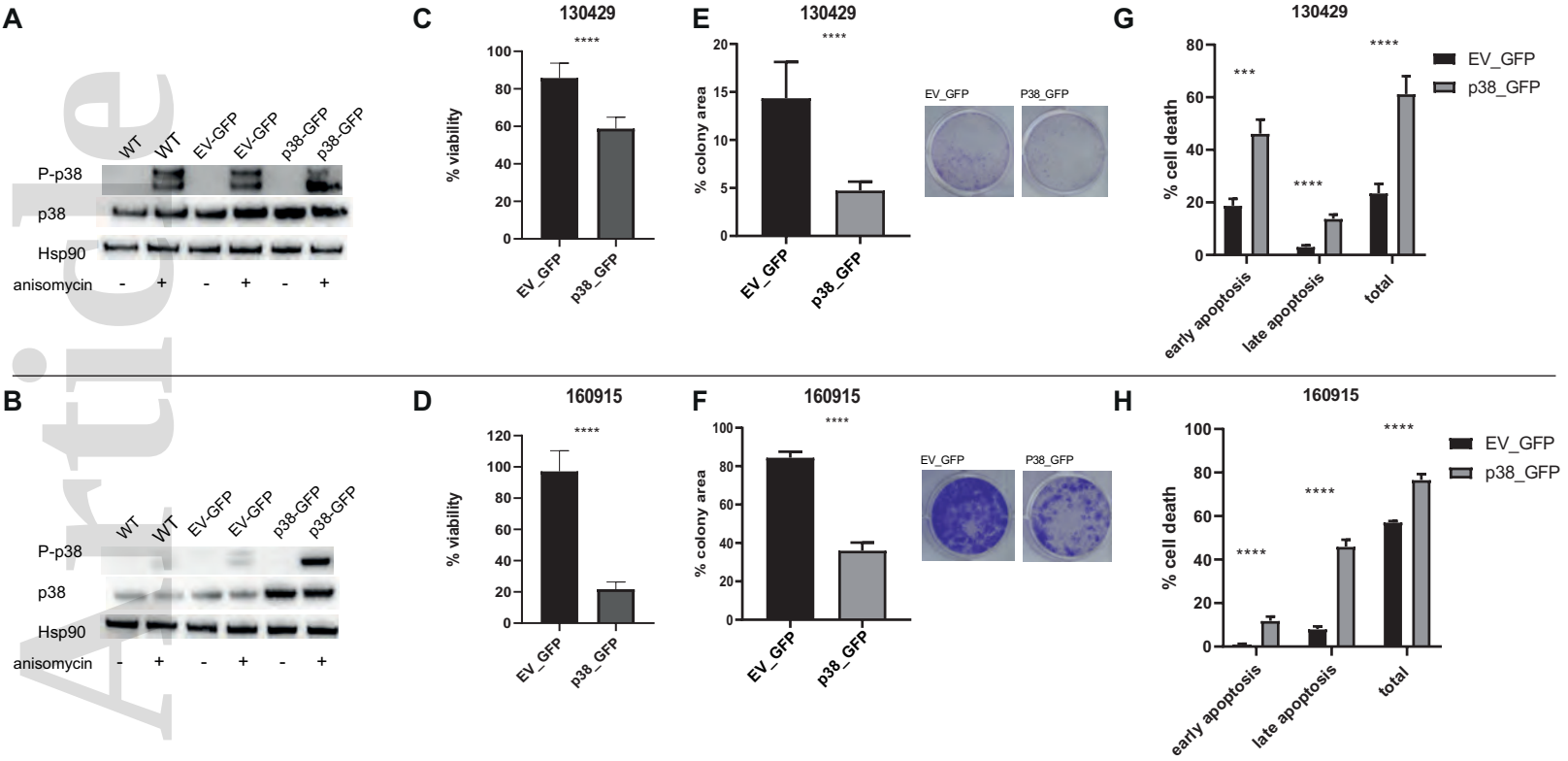

Figure 2: Up-regulation of p38α by stable transfection induces apoptosis mediated cell death resulting in reduced cell viability and clonogenicity in cell line 130429 and 160915

A-B: Relative protein expression of p38α and phospho-p38α in WT, EV_GFP and p38_GFP in 130429 and 160915 respectively. n≥3 independent experiments C-D: Cell lines 130429 and 160915 stably transfected to express p38α have significantly reduced cell viability compared to cells stably transfected to express GFP respectively as measured using Resazurin assay on day 3 . Each data point in C&D represents an average of 30 values per condition per independent experiment. Error bars represent standard error of the mean. Statistical tests done using two tailed unpaired student's t test and significance values indicated are: p≤0.05 *, p≤0.01 **, p≤0.001 * * * E-F: Significant difference (p<0.001) in the area covered by colonies in cell line 130429 and 160915 stably expressing p38α compared to cells stably expressing GFP respectively. Beside are representative pictures of the colonies formed. n≥3 independent experiments. Error bars represent standard error of the mean. Statistical tests done using two tailed paired student's t test and significance values indicated are: p≤0.05 *, p≤0.01 **, p≤0.001 * * *. G-H: Significantly higher population of cells undergoing early, late and total apoptosis in cell line 130429 and 160915 stably transfected to express p38α compared to its mock GFP counterpart respectively. Total apoptosis was calculated as the sum of early, late apoptosis and necrosis. n≥3 independent experiments. Error bars represent standard error of the mean. Statistical tests done using two tailed paired student's t test and significance values indicated are: p≤0.05 *, p≤0.01 **, p≤ 0.001 * * *

pcmr_12925_f2.eps

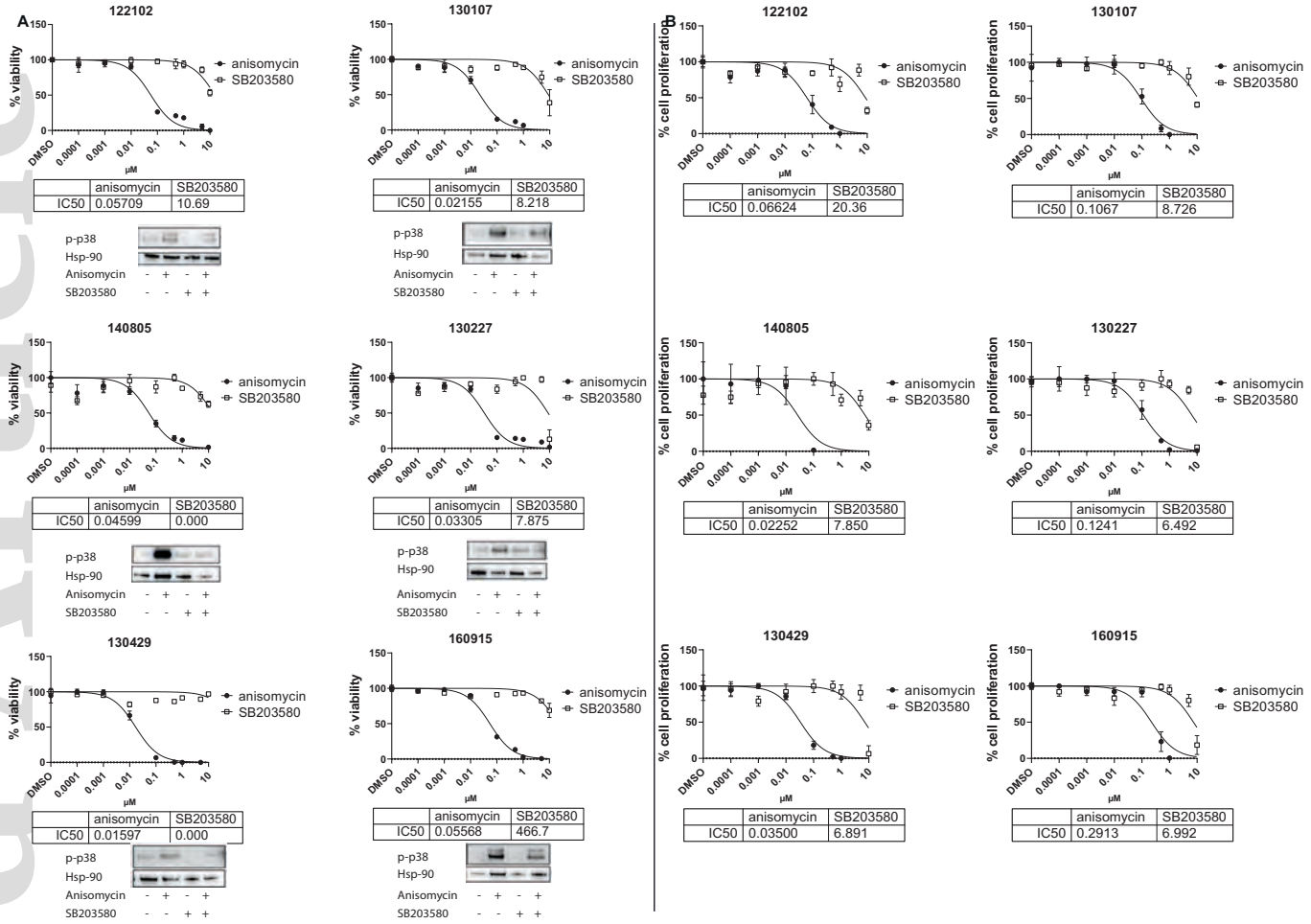

Figure 3: Activation and inhibition of phospho-p38α by anisomycin and SB203580 respectively and reduction in cell viability and proliferation upon anisomycin treatment in all cell lines

A: Resazurin assay showing dose-dependent reduction in cell viability with increasing concentrations of anisomycin but not SB203580 as indicated by the IC50 values (in μM). Each data point represents an average of 3 values per condition per independent experiment. n≥3 independent experiments. Error bars represent standard error of the mean. Below: Western blots showing activation and inhibition of phospho-p38α when stimulated by anisomycin and SB203580 in respective cell lines. B: BrdU colorimetric assay showing dose dependent reduction in incorporation of BrdU with increasing concentrations of anisomycin but not SB203580 as indicated by the IC50 values (in μM). Each data point represents an average of 3 values per condition per independent experiment. n≥3 independent experiments. Error bars represent standard error of the mean.

pcmr_12925_f3.eps

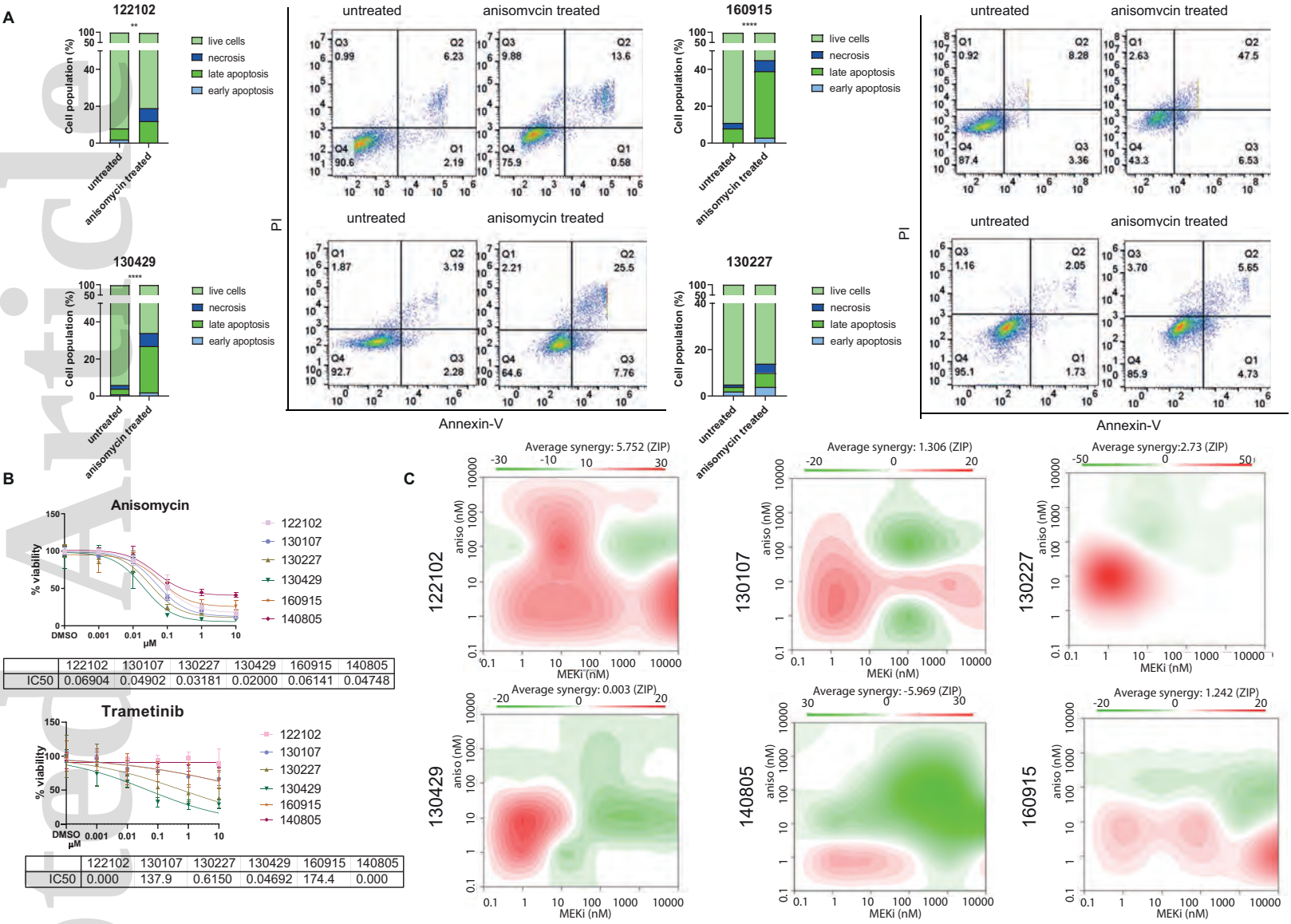

	122102	130107	130227	130429	160915	140805
IC50	0.06904	0.04902	0.03181	0.02000	0.06141	0.04748

	122102	130107	130227	130429	160915	140805
IC50	0.000	137.9	0.6150	0.04692	174.4	0.000

Figure 4: Low dose anisomycin induces apoptosis mediated cell death in NRAS mutant melanoma cell lines and shows synergistic effects with MEK inhibitor-trametinib.
A: Annexin V-PI assay demonstrating significantly higher apoptosis rate in anisomycin (0.1 μM) treated 122102, 130429, 160915 compared to untreated cells. Anisomycin (0.1 μM) treated 130227 had 10% higher apoptosis compared to untreated cells. Below: Separation of untreated and anisomycin treated cells into early apoptosis Q1, late apoptosis Q2, necrosis Q3 and live cells Q4. Error bars represent standard error of the mean. n≥3 independent experiments. Statistical tests done using Chi-squared test and significance values indicated are: p≤0.05 *, p≤0.01 **, p≤0.001 * * * B: Resazurin assay upon dose dependent treatment with anisomycin/trametinib. Sensitivity to the drug is measured by IC50 value in the table below. Each data point represents an average of 3 values per condition per independent experiment. n≥3 independent experiments. Error bars represent standard error of the mean. Undetermined IC50 is indicated by 0.000 C: Synergy plots of 122102, 130107, 130227, 130429 , 140805 and 160915 treated with trametinib (concentrations on x-axis) and anisomycin (concentrations on y-axis). Red, white and green indicate synergistic,non- synergistic and antagonistic effects respectively. Each data point represents an average of 3 values per condition per independent experiment. n>3 independent experiments.

pcmr_12925_f4.eps

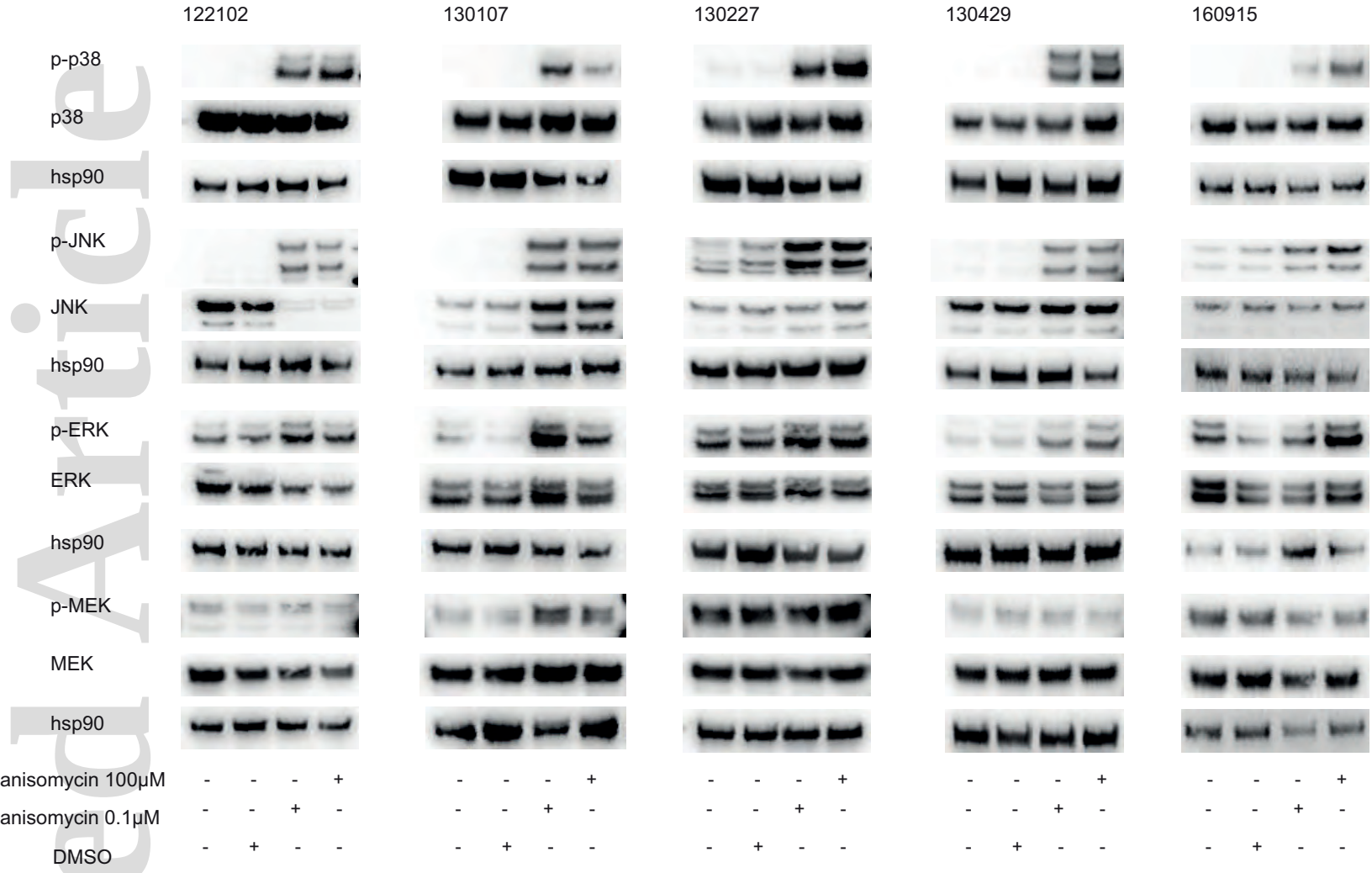

Figure 5: Anisomycin upregulates phospho-JNK along with phospho-p38α and JNK inhibitor SP600125 can suppress anisomycin induced p38α activation
Relative protein level expression of 122102, 130107, 130227, 130429 and 160915 under high (100 μM) and low (0.1 μM) dose anisomycin probed for phospho-p38α/p38α, phospho-JNK/-JNK, phospho-ERK/ ERK and phospho-MEK/ with hsp90 as loading control.

pcmr_12925_f5.eps

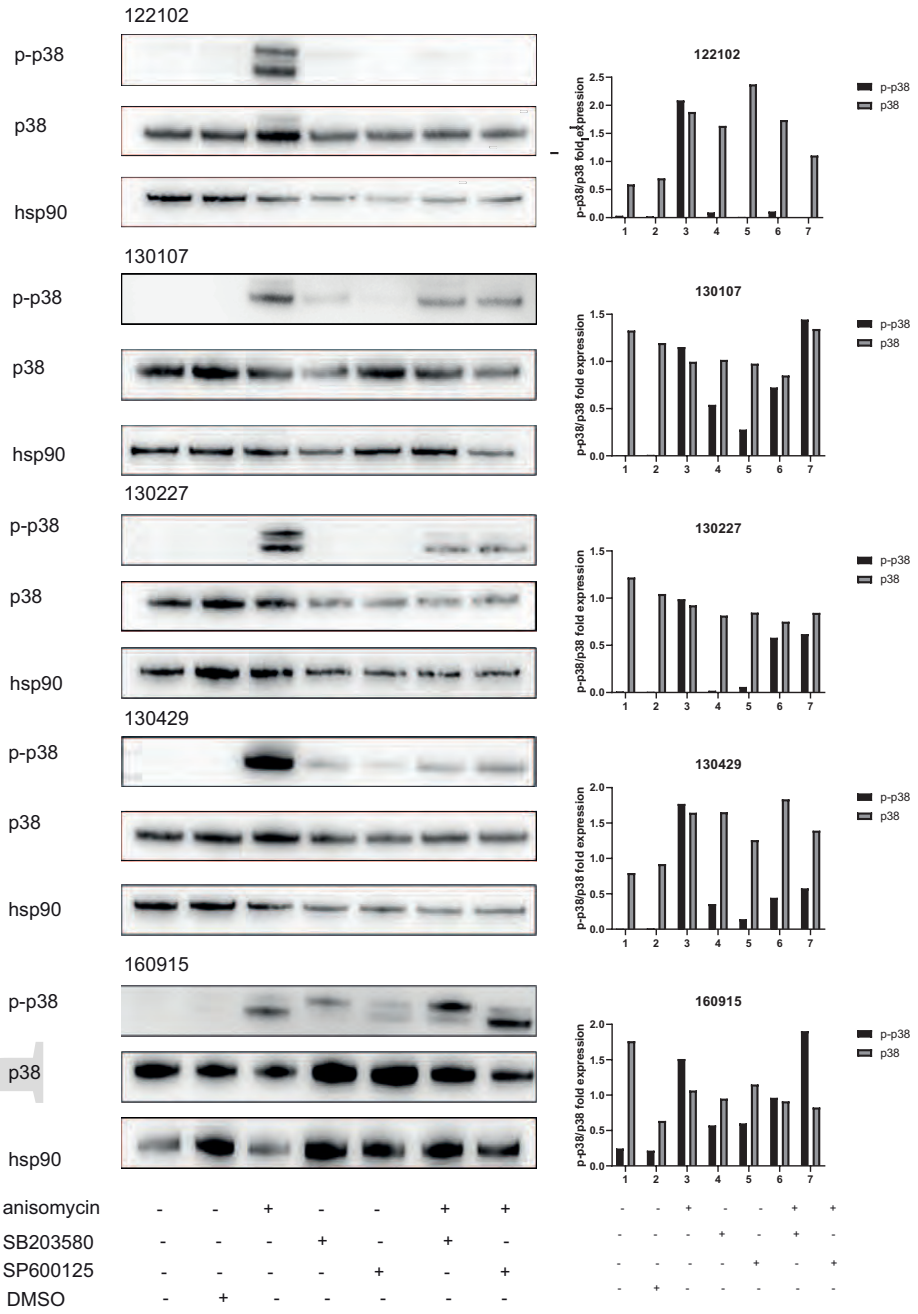

Figure 6: p38 inhibitor-SB203580 and JNK inhibitor-SP600125 can suppress anisomycin induced p38α activation
Relative protein level expression of 122102, 130107, 130227, 130429 and 160915 under low (0.1 uM) dose anisomycin probed for phospho-p38α/p38α with hsp90 as loading control. Phospho-p38α levels were reduced when co-treated with anisomycin and SP600125 in 122102, 130227 and 130429 while phospho-p38α levels were reduced when co-treated with anisomycin and SB203580 in 122102,130107, 130227, 130429 and 160915. 130107 and 160915 had higher expression of phospho-p38α when co-treated with anisomycin and SP600125. On the right: Fold expression of p38α and phospho-p38α normalized to hsp90.